Received: 30 August 2023 | Revised: 01 October 2023 | Accepted: 08 October 2023
DOI: 10.48309/jmpcr.2023.182241
Journal of Medicinal and Pharmaceutical Chemistry Research
SAMI

FULL PAPER

Fabrication and analysis of nano-hydroxyapatite [$Ca_{10}(PO_4)_6(OH)_2$] composites with collagen derived from eggshells through freeze-drying

Maming Maming[a] |Fadliah Mubakira[a] |Indah Raya[a,*] |Bulkis Musa[a] |Andi Muhammad Anshar[a] |Erna Mayasari[a] |Yusafir Hala[a] |Syaharuddin Kasim[a] |Andi Ilham L.[b] |Gemini Alam[c] |Andi Nilawati Usman[d] |Hasmawati Hasmawati[e] |Hasri Hasri[f] |Andriani Usman[a] | Rizal Irfandi[f,g]

[a]*Department of Chemistry, Faculty of Mathematics and Natural Science, Hasanuddin University, Makassar 90245, Indonesia*

[b]*Department of Biology, Faculty of Mathematics and Natural Sciences, Hasanuddin University, Makassar, Makassar 90245, Indonesia*

[c]*Faculty of Medicine, Hasanuddin University, Makassar, Makassar 90245, Indonesia*

[d]*Midwifery Study Program, Hasanuddin University, Makassar 90245, Indonesia*

[e]*Department of Matematics, Faculty of Mathematics and Natural Sciences, Hasanuddin University, Makassar 90245, Indonesia*

[f]*Department of Chemistry, Faculty of Mathematics and Natural Science, Universitas Negeri Makassar, Makassar 90244, Indonesia*

[g]*Department of Biology Education, Faculty of Teacher Training and Education, Universitas Puangrimaggalatung, Sengkang 90915, Indonesia*

***Corresponding Author:**
Indah Raya
E-mail: indahraya@unhas.ac.id
Tel.: + 089695544909

This study aims to know how to composite hydroxyapatite-collagen by freeze-drying method, and the characterization of hydroxyapatite-collagen composites using XRD, FTIR, and SEM. Hydroxyapatite nanocrystals are synthesized using the precipitation method by reacting CaO and $(NH_4)_2HPO_4$ and the freeze-drying method in composite manufacturing by reacting hydroxyapatite nanocrystals with collagen. The results showed that hydroxyapatite nanocrystals can be composite with collagen using the freeze-drying method, and the results of characterization of XRD, FTIR, and SEM hydroxyapatite-collagen composites show the formation of chemical bonds between hydroxyapatite and collagen. The XRD spectrum of HAp-Collagen shows a peak at 2θ 10.45°, showing a physically formed composite. FTIR characterization shows the presence of absorption bands PO_4^{3-} and OH^- from HA, slight wavenumber shifts also occur in C-H, C-N, N-H, and C=O groups which are characteristic of collagen, this indicates that composites are formed physically. SEM characterization shows HAp is perfectly deposited into collagen molecules.

KEYWORDS

Eggshell; bone repair; hydroxyapatite-collagen composite; nano hydroxyapatite.

Introduction

The bone damage cases continue to increase every year, this is triggered by age factors and unhealthy diets, congenital and non-congenital diseases, and rampant cases of accidents and natural disasters [1]. Researchers believe that the use of natural materials in the manufacture of bone substitution biomaterials is more acceptable to the body because of the similarity of physicochemical properties with actual bone [2,3]. Hydroxyapatite (HAp) material is the main component of bone minerals and part of the apatite mineral group, with the chemical formula $Ca_{10}(PO_4)_6(OH)_2$. HAp is one of the calcium phosphate compounds. It is a ceramic material with chemically stable properties

when compared to metal and polymer materials [4].

HAp synthesis material in this study used eggshells as a source of calcium because eggshells contain around 94-97% $CaCO_3$ and the potential for this waste in Indonesia is quite large. According to data from the Directorate General of Livestock in 2016, egg production of laying and free-range chickens in Indonesia in 2015 amounted to 1,481,481 tons per year. About 10% of eggshells so around 148,148 tons of eggshells are produced per year [5,6]. Eggshells have the main composition of $CaCO_3$ which can cause pollution due to microbial activity in the environment. The eggshell consists of 4 different layers, namely (from the inside out) the membrane layer, the mammillary layer, the foam layer, and the cuticle layer [7]. The chicken eggshell that wraps the egg weighs 9-12% of the total egg weight and contains 94% calcium carbonate, 1% potassium phosphate, and 1% magnesium carbonate [8]. The availability of calcium from eggshells is quite high, which is 93.80% [9] so it has the potential to be used in synthesizing hydroxyapatite.

This research uses precipitation methods that have been widely applied to make HAp because it is simple, economical, and easy to do. There are two different crystal structures in HAp, monoclinic and hexagonal. According to [10] hydroxyapatite structure obtained only under pure conditions and stoichiometric composition (Ca/P ratio 1.67), this structure has good thermal stability. HAp is found in teeth and bones and the mineral HAp is hexagonal, except in tooth enamel with monoclinic structures [11].

Bone consists of collagen and hydroxyapatite as the main component and a few percent of other components, to make bone graft as a substitute for bone whose composition is similar to bone, HAp biomaterial powder needs to be composite with collagen because collagen protein is able to stimulate the growth of new bone cells and is biocompatible with the body and biodegradable [12].

In this study, the objective is how to fabricate hydroxyapatite-collagen composite by freeze-drying method. Hydroxyapatite-collagen composite is characterized by XRD, FTIR, and SEM.

Experimental

Synthesis of Hydroxyapatite Compounds

Calcination and Synthesis of Calcium Oxide from Chicken Eggshells)

Eggshell waste is cleaned with aqueous and dried at room temperature. The dried eggshells are then mashed using a mortar and sifted using a 100-120 mesh sieve to obtain an average clamshell particle size of 0.125-0.15 mm.

Egg shells that have been mashed to a size of 0.125-0.15 mm are then calcined using a furnace at a temperature of 1000 ºC for 5 hours to remove organic components and converted calcium carbonate ($CaCO_3$) into calcium oxide (CaO). CaO was then analyzed for calcium levels using XRF, and then XRD and FTIR characterization was carried out.

Preparation of Calcium and Phosphate Solutions

CaO powder that has been weighed according to stoichiometric calculations, dissolved with HNO_3(p). After that, equates up to 100 mL are added. The pH of the solution is set at pH 10 by adding ammonium hydroxide (NH_4OH) and buffer. Almost similar treatment is also carried out in making phosphate solutions. Crystals $(NH_4)_2HPO_4$ that have been weighed are dissolved with aquabides up to 100 ml then the pH of the solution is set at pH 10 and a buffer is added.

Hydroxyapatite synthesis

Synthesis was carried out using the precipitation method, namely a solution of $(NH_4)_2HPO_4$ 0.3 M as much as 100 mL inserted drop by drop into a suspension of CaO at 40 °C (kept constant) while the solution was stirred with a magnetic stirrer at a speed of 300 rpm for 60 minutes. After precipitation is complete, aging is carried out (stored) for 24 hours. The precipitate formed is then filtered to be separated by a supernatant using Whatman 42 filter paper and then washed with aqua bides to remove residual ammonium nitrate. The precipitate is then dried at 110 °C for 5 hours. Furthermore, sintering is carried out on a dry precipitate to obtain $Ca_{10}(PO_4)_6(OH)_2$ compounds at 800 °C for 1 hour. After that, characterization was carried out on $Ca_{10}(PO_4)_6(OH)_2$ compounds produced using XRD, FTIR, and SEM.

Characterization by electron microscopy (SEM) spectroscopy

The characteristics of using SEM are carried out to determine the surface morphology of collagen (Bovine Collagen Peptide). The tool used by SEM model Tescan Vega 3 Bruker at the Scanning Electron Microscope Laboratory FMIPA ITB, Bandung. The sample was placed on an aluminum plate that had two sides and then coated with a layer of gold 48 nm thick. Coated samples were observed using SEM with a voltage of 22 kV and magnifications of 20,000x and 40,000x.

Synthesis of hydroxyapatite-collagen nanocomposite

The synthesis of hydroxyapatite-collagen composites by freeze-drying method begins with the mixing of hydroxyapatite and collagen with a composition ratio of 67:33. The composite manufacturing method refers to the method of [13] with modifications. Before the two ingredients are mixed, collagen and hydroxyapatite are dissolved first to obtain a homogeneous mixture. Collagen is dissolved in 1M acetic acid then added $Na_2HPO_4.2H_2O$ in a ratio of 1: 1: 1. This acidic solution is neutralized by adding 1M NaOH. Hydroxyapatite is dissolved in phosphoric acid in a ratio of 1:4, neutralized with NH4OH drop by drop with a glass pipette. Neutral pH is measured using universal pH paper. The collagen solution and hydroxyapatite solution are then mixed and stirred slowly for 15 minutes. The solution is precipitated ±6 hours. The liquid above the precipitate is discarded, and the precipitate is poured in a petri dish and labeled. Then frozen at -40 °C with a freezing time of 24 hours. The dried collagen-hydroxyapatite composite was then characterized using XRD, FTIR, and SEM.

Characterization with X-Ray Diffraction (XRD)

Characterization using XRD is performed for phase identification, crystal structure, degree of crystallinity, and crystallite size of the sample. The XRD tool used is XRD-7000 Maxima-X Shimadzu in the Integrated Laboratory of Science Building MIPA Unhas, CuKα target source (λ= 1.54056 Angstrom). The sample to be characterized is previously ground into a fine powder measuring > 2 μm, and then pelletized and placed on preparation. The preparation is then placed on a sample holder X-ray diffractometer for further analysis with XRD.

Characterization with fourier transform infra-red (FTIR)

Characteristics with FTIR are carried out to determine the functional groups contained in the sample. Precipitates that have been dried and ground into powder are characterized using the FTIR spectroscopy model Shimadzu 820 1 PC at the Integrated Chemistry Laboratory of the Department of Chemistry, FMIPA Unhas. Two milligrams of precipitate are mixed with 100 mg KBr, and printed into thin discs or pellets, then tested with a

wavenumber range of 4000-400 cm^{-1}; KBr is always included on each measurement to eliminate background absorption.

Characterization by electron microscopy (SEM) spectroscopy

Characteristics using SEM are carried out to determine the surface morphology of the sample. The tool used by SEM model Tescan Vega3 Bruker at the Scanning Electron Microscope Laboratory FMIPA ITB, Bandung. The sample was placed on an aluminum plate that had two sides and then coated with a layer of gold 48 nm thick. Coated samples were observed using SEM with a voltage of 22 kV and magnifications of 20,000x and 40,000x.

Results and discussion

Eggshell calcination

The synthesis of $Ca_{10}(PO_4)_6(OH)_2$ begins by calcining the eggshell. Calcination carried out on eggshells aims to eliminate organic components and convert calcium carbonate compounds ($CaCO_3$) into calcium oxide CaO which is used as a precursor to calcium (Ca).

At the calcination stage, the process of decomposition of the eggshell occurs. At temperatures below 250 °C water will evaporate then all organic components will oxidize below 450 °C. At 540 °C, there is decomposition of magnesium carbonate ($MgCO_3$) and $CaCO_3$ is converted to CaO at about 750 °C. The complete decomposition of $CaCO_3$ to CaO occurs at 1000 °C [14]. In this study eggshell calcination was carried out at the optimum temperature and time of 1000 °C for 5 hours referring to [15], to eliminate organic components and convert $CaCO_3$ compounds into CaO through the elimination of CO_2 in gas form, which can also be seen from mass reduction after calcination. As for the results of the reaction:

$$CaCO_3(s) \rightarrow CaO(s) + CO_2(g)$$

Identification of CaO before and after calcination of chicken eggshells by X-ray diffraction (XRD) analysis

XRD analysis aims to determine the structure and crystal phase of the calcined CaO sample of chicken eggshells and ensure that $CaCO_3$ in the eggshell has turned into CaO. In the picture, it appears that there is a change in the diffraction pattern of eggshells after calcination. The X-ray diffraction pattern undergoes peak reduction and narrowing indicating the conversion of $CaCO_3$ to CaO and the release of CO_2 gas. The X-ray diffraction pattern in Figure 1 is monitored at 2θ = 20-70º. The XRD pattern of eggshells before calcination shows characteristic peaks of $CaCO_3$ at 2θ = 29.77 °, 47.9°, and 39.75°.

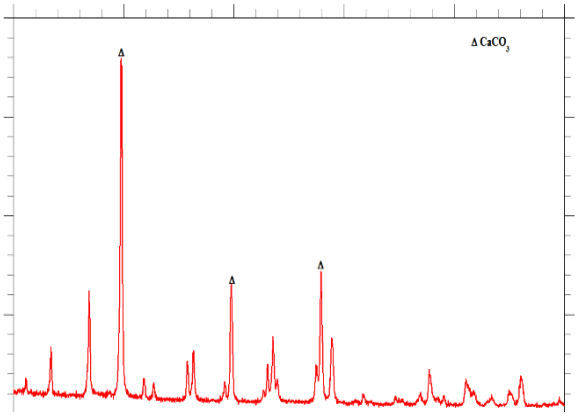

(a)

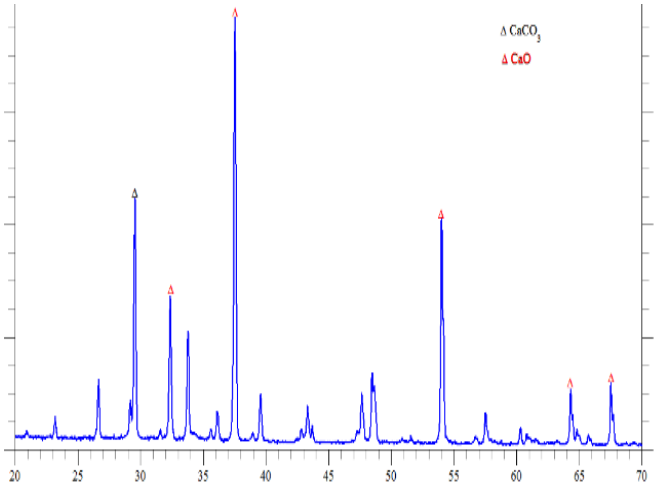

(b)

FIGURE 1 XRD diffraction pattern of chicken eggshells (a) before calcination and (b) after calcination at 1000 °C for 5 hours

The diffraction pattern calcined by chicken eggshells in Figure 1 was matched with the pure CaO diffraction pattern from the Joint Committee on Powder Diffraction Standards (JCPDS) as a comparison. The compound content can be analyzed through 2θ observations, as presented in Table 1.

TABLE 1 Data on 2θ CaO compounds from JCPDS as well as calcined results of chicken eggshells

Sample	T(°C)	2θ (°)				
JCPDS	-	32,2	37,35	53,86	64,15	67,38
Chicken Egg Shell	1000	32,59	37,75	54,25	64,54	67,76

In the diffraction pattern data from the calcination of chicken egg shells at a temperature of 1000 °C, a crystalline CaO structure is produced which is indicated by the appearance of sharp peaks indicating an increase in the crystallinity of the resulting CaO, but there is still a diffraction pattern associated with the $CaCO_3$ phase that appears at 2θ (°) = 29.38 along with the presence of several CaO peaks at 2θ (°) = 32.59; 37.75, 54.25, 64.54, and 67.76. These peaks correspond to results published by Albuquerque for diffraction patterns of CaO with cubic structures [16].

The diffraction pattern of $CaCO_3$ that appears can be due to the condition of the sample that is open when characterized XRD so as to allow the formation of $CaCO_3$ through the absorption of CO_2 from the atmosphere during XRD analysis [17,18]. Revealed that CaO can react with CO_2 slowly at room temperature to form $CaCO_3$. The reaction can be written in the following equation:

$$CaO_{(s)} + CO_{2(g)} \rightarrow CaCO_{3(s)}$$

Also mentioned that the size of CaO particles greatly affects the absorption capacity of CO_2, where the smaller the size of CaO, the greater the absorption power of CO_2 due to the larger surface area.

Identification of CaO before and after calcination of chicken eggshells with FTIR spectrophotometer

Characterization by infrared spectroscopy aims to identify functional groups present in a compound. Figure 2 depicts the FTIR spectra of CaO synthesis after calcination at wavenumbers between 4000-250 cm^{-1}. The identification results showed the elimination of CO_2 and organic components.

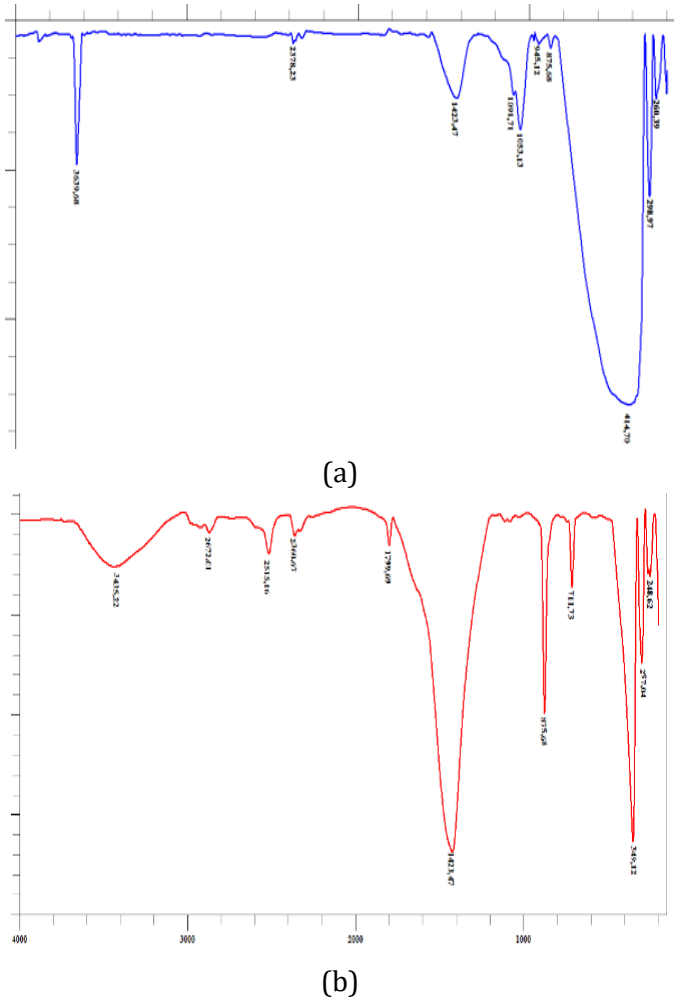

FIGURE 2 FTIR characterization results: (a) eggshell after calcination and (b) eggshell before calcination

The Ca-O absorption band in chicken egg shell samples was seen in the area of 414.70 cm^{-1} which showed the vibration of Ca-O from calcined metal oxides. This band is strengthened by the appearance of peaks in waves 1053.13 cm^{-1} and 1091.71 cm^{-1} which are the bending vibrations of carbonate groups [19].

The band at wavenumber 1423.47 cm^{-1} corresponds to the bidentate and monodentate species of carbonate. This is in accordance with research conducted by [19], that the band at wavenumber 1423.47 cm^{-1} can be interpreted as *vibrational stretching* asymmetry of the O-C-O bond of carbonate monodentate on the CaO surface.

The band with a sharp peak at wavenumber 3639.68 cm^{-1} is the extended vibration of the OH group of $Ca(OH)_2$. The presence of OH groups may come from water molecules adsorbed on the CaO surface because CaO is hygroscopic so it is very easy to absorb water vapor from the air [19].

Identification of calcined Ca levels of chicken eggshells with XRF (X-Ray Fluorescence)

XRF (X-Ray Fluorescence) Spectrometry analysis aims to identify and determine the concentration of elements present in the calcination of chicken egg shells. Based on the analysis of calcination results, CaO levels of 99.35% were obtained which can be seen in the Table 2.

TABLE 2 Identification of Calcined Ca levels of chicken eggshells

Component Compound	Value (%)	Component Compound	Value (%)
CaO	99,35	Ca	71,03
P_2O_5	0,572	P	0,249
Nb_2O_5	0,0238	Nb	0,0166
MoO_3	0,0188	Mo	0,0125
RuO_4	0,0080	Ru	0,0061
In_2O_3	0,0072	In	0,0060
SnO_2	0,0064	Sn	0,0050
Sb_2O_3	0,0062	Sb	0,0052
TeO_2	0,0057	Te	0,0046
Rh_2O_3	0,0053	Rh	0,0043

Precipitation reactions with phosphate precursors

The results of CaO calcination measured calcium levels using *X-Ray Fluorescence* so that calcium levels were obtained after calcination, which was 71.03%. These results are then used for stoichiometric calculations in determining the amount of calcined CaO needed to react with phosphate precursors $(NH_4)_2HPO_4$ to produce $Ca_{10}(PO_4)_6(OH)_2$, at the optimum stirring reaction temperature of 40 °C for 1 hour referring to [20]. Heat treatment was carried out to study the effect of temperature changes on particle size and crystallinity of hydroxyapatite synthesis. The sample from the dry precipitate then interacted at the optimum temperature of formation $Ca_{10}(PO_4)_6(OH)_2$ which is 800 °C for 1 hour referring to [15] to obtain pure HAp. Furthermore, the characterization of hydroxyapatite from synthesis was carried out using XRD, FT-IR, and SEM data.

Characterization of sintering results with XRD

Characterization with XRD aims to identify the structure and crystalline phase of calcium phosphate compounds present in the material that has been synthesized. The XRD characterization pattern can be seen in Figure 3.

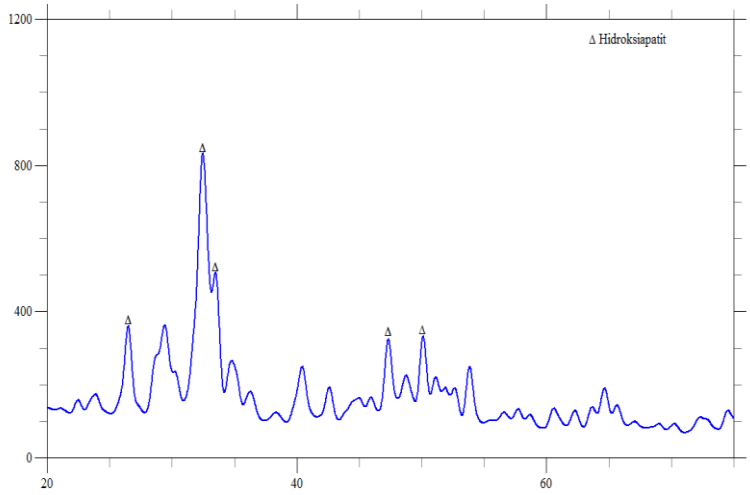

FIGURE 3 Diffraction pattern $Ca_{10}(PO_4)_6(OH)_2$ synthesized at sintering temperature 800 °C

The results obtained were compared with the intensity of the peaks on the measured diffractogram with the database, the synthesized Ca $10(PO_4)_6(OH)_2$ compound was matched with JCPDS (*Joint Committee on Powder Diffraction Standards*) standard data, the results showed that the calcium phosphate compound contained in the synthesis result was a hydroxyapatite compound with a purity of 60.9%.

TABLE 3 The peak position of XRD HAp eggshell synthesis that has been analyzed against HAp stoichiometry data JCPDS (*Joint Committee on Powder Diffraction Standards*)

	Crystal plane (h k l)					
	(002)	**(211)**	**(300)**	**(202)**	**(310)**	**(222)**
HAp synthesis	25.88	31.86	32.89	34.36	39.86	46.32
JCPDS	25.879	31.738	32.864	34.048	39.818	46.661

In Table 3, there is a slight difference between HAp synthesis from eggshells and HAp JCPDS, but it can be concluded that HAp synthesis from eggshells has almost the same characterization and elements and resembles standard HAp, from Figure it can be concluded that the dominant peak is at 32.4943°, the second dominant peak is 33.5000 and the third dominant peak is at 26.4821 which shows the character of $Ca_{10}(PO_4)_6(OH)_2$.

Characterization of sintering results with FT-IR (Fourier Transform Infra-Red)

Characterization by infrared spectroscopy aims to identify functional groups present in a compound. The results of FTIR (Fourier Transform Infra-Red) characterization show that the sintering sample contains a dominant compound in the form of HAp. The characterization pattern of FTIR spectra can be seen in Figure 4.

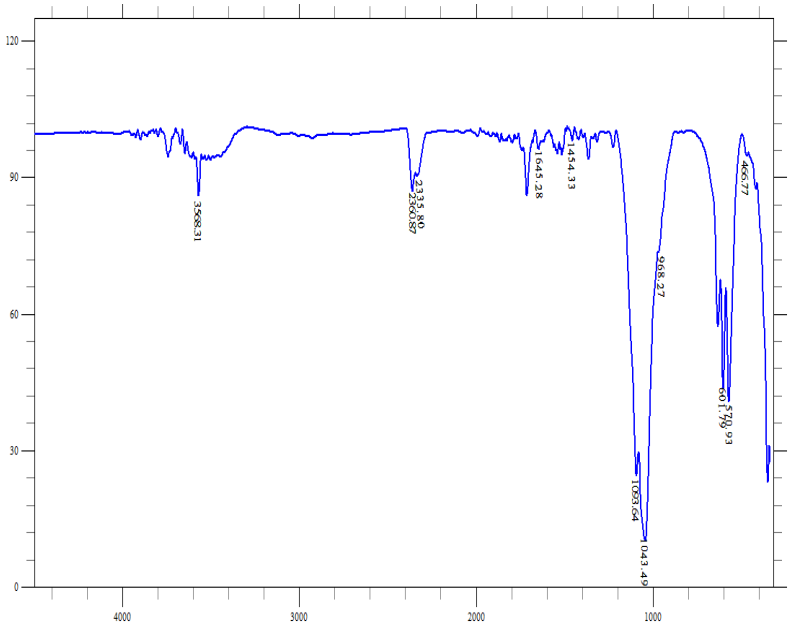

FIGURE 4 FTIR spectroscopic spectroscopy $Ca_{10}(PO_4)_6(OH)_2$ synthesis at sintering temperature 800 ^oC

The FTIR results reinforce the assumption that overall, the dominant compound formed is HAp. Overall, the absorption spectrum of PO_4^{3-} for symmetrical stretching vibrations (υ_1) and symmetrical *bending* vibrations (υ_2) is in the absorption area of 962-970 cm^{-1} and 466-472 cm^{-1}, asymmetrical *stretching* vibrations (υ_3) are in the absorption area of 1041-1093 cm^{-1}, while for vibrations Asymmetric bending (υ_4) indicates the presence of two split absorption bands in the regions of 570 cm^{-1} and 603 cm^{-1} indicating the presence of HAp crystals [21].

The FTIR spectra above have indicated the presence of phosphate ions (PO_4^{3-}), hydroxyl (OH^-), and carbonate (CO_3^{2-}). Overall, the absorption spectrum of PO_4^{3-} for symmetrical stretching vibrations (υ_1) and symmetrical

bending vibrations (υ_2) was in the absorption area of 968.27 cm^{-1} and 466.77 cm^{-1}, asymmetrical *stretching* vibrations (υ_3) were in the absorption area of 1043.49 cm^{-1}, 1093.64 cm^{-1}, while for asymmetric bending vibration (υ_4) it was shown the presence of two absorption bands in the area of 570.93 cm^{-1} and 601.79 cm^{-1} indicating the presence of HAp crystals. The presence of a free OH^- group in the absorption area of 3568.31 cm^{-1} also indicates the presence of HAp compounds.

In addition, absorption in the areas of 1645.28 cm^{-1} and 1454.33 cm^{-1} indicates the presence of carbonate groups (CO_3^{2-}) in very small amounts (*trace elements*), which indicates that the synthesized HAp still contains carbonates. The presence of carbonate in the HAp structure is considered not good because it can reduce its thermal stability; therefore, the presence of carbonate needs to be eliminated by inserting the conditions at the time of the precursor mixing reaction [22].

Characterization of Nano Hydroxyapatite by Electron Microscopy (SEM) Spectroscopy and Energy Dispersive X-Ray Spectrometer (EDS)

Characterization Sample

Nano HAp result synthesis uses Spectroscopy Electron Microscopy (SEM) aims to identify from size, shape, structure, and morphology of nanocrystal HAp that formed, as demonstrated in Figure 5.

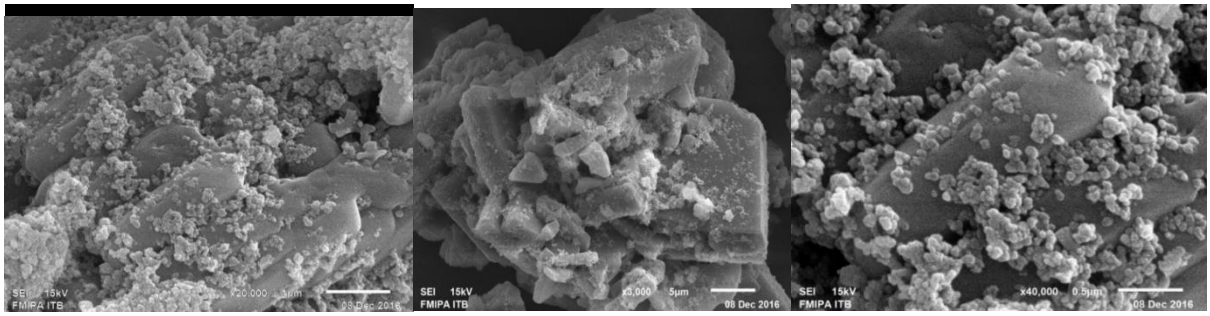

(a) (b) (c)

FIGURE 5 Morphology of nano HAp SEM test results (a) magnification 3,000x, (b) magnification 20,000x, and (c) 40,000x magnification

Hydroxyapatite is generally made in powder form and if visually observed it will appear that the hydroxyapatite powder is composed of fine grains. In Figure 5, the SEM characterization show that the constituent particles of hydroxyapatite synthesis are in the form of fine grains that are not uniform and vary resembling the shape of crystals collected in agglomerates, the arrangement and distance of the constituent particles of hydroxyapatite samples are also irregular. While [23], reported that the morphology of commercial hydroxyapatite in the form of granules that form aggregates, the size of the granules is uneven and has a smooth structure.

Revealed that particle agglomeration occurs through several stages, namely (a) nucleation and particle growth in the nano order, (b) particle aggregation due to physical interaction, and (c) crystal growth at constant residual super saturation [20].

Furthermore, the microstructure of hydroxyapatite has various sizes and is influenced by the treatment temperature used [24,25]. Given that the morphology of hydroxyapatite that has undergone a heating process in the form of crystals and the crystals are irregular, it is suspected that it increases with the increase in temperature used from the SEM image shown showing photos of HAp electron microscopes with magnifications of 3,000 times, 20,000 times and 40,000 times. It

is clear in the figure that HAp is composed of crystals with small sizes in the nano order (50-100 nm) and the surface of this hydroxyapatite compound tends to be smooth and non-porous. HAp with nanoparticles is very useful as a bone substituent because bones are composed of inorganic components, especially HAp with crystalline nanostructures. In addition, nanocrystals will be more easily absorbed by the body because they have a large surface area.

EDS is one of the tools assembled on the SEM tool. EDS analysis produces qualitative and quantitative information about the composition of the locations in the sample with a diameter of several micrometers. To determine the content of Ca and P possessed in the synthesized hydroxyapatite sample, EDS characterization was carried out. Figure 6 illustrates the synthesis composition dominated by oxygen (O) up to 61.42% followed by calcium (Ca) up to 21.16% and phosphorus (P) 17.42%. This composition corresponds to the composition of hydroxyapatite.

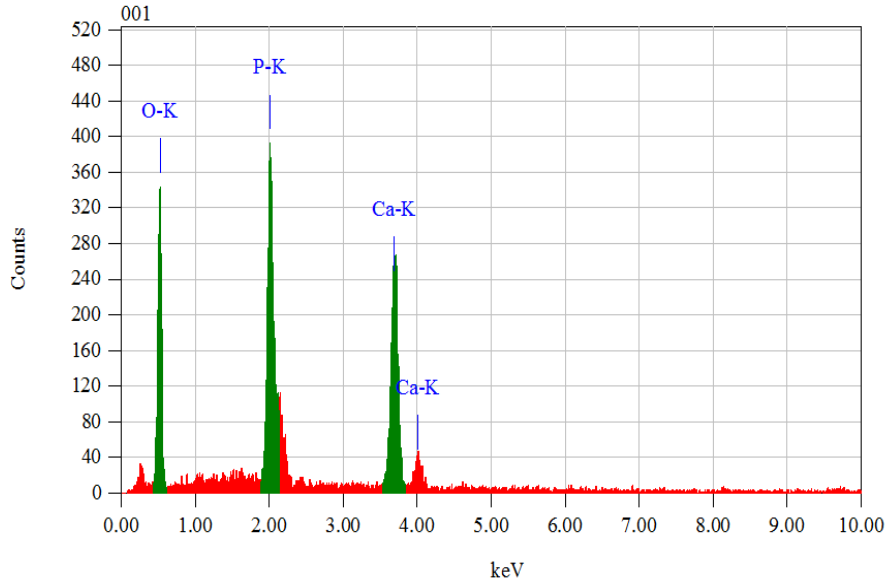

FIGURE 6 EDS nano HAp synthesis results

The Ca/P molarity ratio is obtained by EDS measurements performed in conjunction with SEM characterization. The Ca/P ratio to HAp is 1.67. The Ca/P ratio obtained is relatively slightly smaller. The value of the Ca/P ratio obtained can be influenced by the emergence of carbonate groups as seen from the results of FTIR and XRD analysis. The presence of this carbonate will affect the amount of Ca and P in the sample, so the ratio obtained is not exactly 1.67. The Ca/P ratio is obtained by comparing the percentage of mass divided by the relative mass of Ca and P so that a molarity ratio between Ca and P will be obtained.

Characterization of Collagen (Bovine Collagen Peptide)

Characterization of Collagen with XRD

XRD characterization is carried out to determine the phase formed in the sample, the degree of cristanility of the sample, crystal lattice parameters, and the crystal size of the sample. The analysis was conducted by matching JCPDS (Joint Committee on Powder Diffraction Standards) data. The following is the XRD pattern of collagen (Bovine Collagen Peptide) samples.

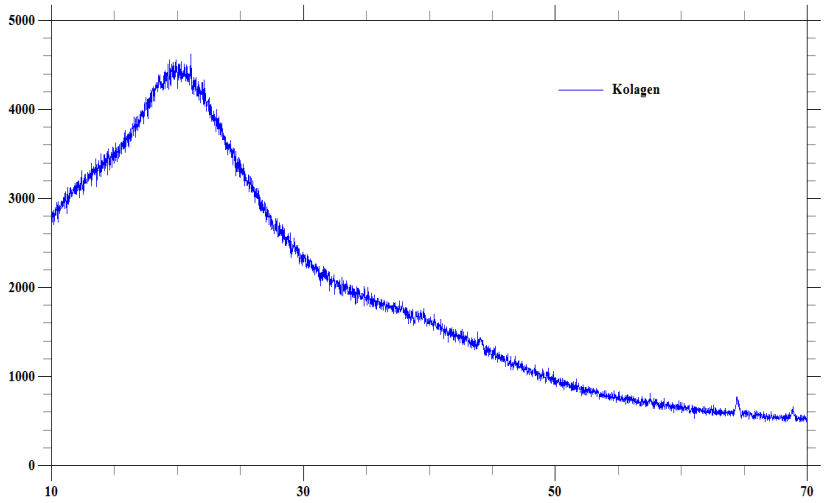

Figure 7 XRD diffraction pattern of collagen (*Bovine Collagen Peptide*) samples

Figure 7 shows the XRD pattern formed in a sample of collagen (*Bovine Collagen Peptide*). The collagen XRD pattern shows characteristic peaks at 2θ = 19.9°. From this pattern, it can also be seen that collagen samples have a mixed structure between crystalline and amorphous.

Characterization of Collagen with FT-IR (Fourier Transform Infra-Red)

The results of FTIR spectrum analysis of collagen (*Bovine Collagen Peptide*) in the form of yellowish-white powder appear on the transmission graph (%) to the wavenumber (cm-1) in Figure 8. Before being tested, samples of collagen powder mixed with potassium bromide (KBr) were then crushed with mortar to remove the scattering effect of large crystals. The sample has been smooth and evenly pressed mechanically to form a translucent pellet so that it can pass through the infrared spectrum.

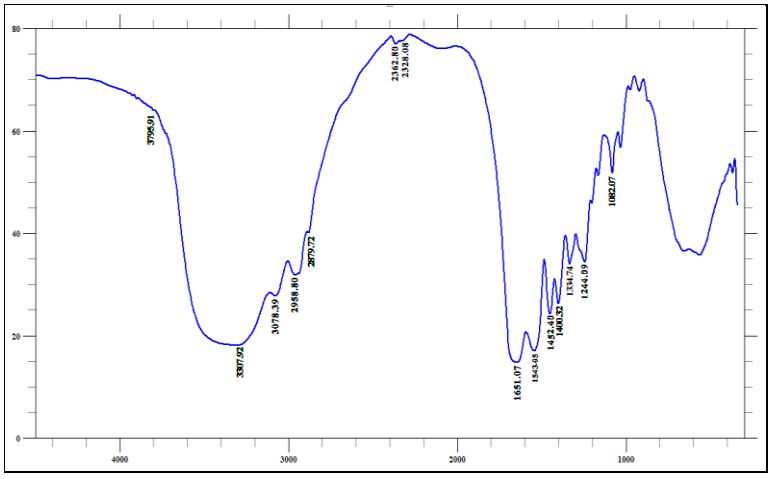

FIGURE 8 Spectroscopy of Collagen powder FTIR (*Bovine Collagen Peptide*)

Functional group analysis was performed by comparing the absorbing bands formed in the infrared spectrum using a correlation table and using the spectra of comparison compounds already known in Figure 9.

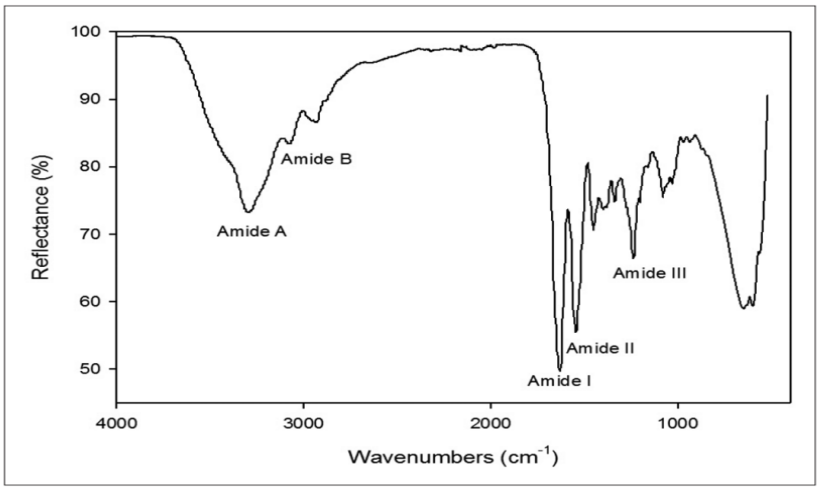

FIGURE 9 Spectroscopic spectroscopy spectrum of pure Collagen FTIR Comparator [26]

The result analysis of spectrum FTIR Collagen from *bovine collagen peptide* proves that Spectrum main from Collagen be the presence of amide I appeal the appearance from stretching vibration C=O (carbonyl) group amide from Protein that is consisted of cluster amide that absorbing N-H stretching at Numbers wave 3307.92 cm^{-1} and 1543.05 cm^{-1}, C=O stretching at numbers wave 1651.07 cm^{-1}, C-N stretching vibration at 1244,09 cm^{-1}, and C-H stretching at 1452,40 cm^{-1} and 1400.32 cm^{-1}. Besides that, exist cluster hydroxyl (-OH) on numbers wave 3078.39 cm^{-1}. The Data show cluster function that is appropriate with structure Collagen so that get concluded that *bovine collagen peptide* succeeds in Synthesized and gets used as material for Synthesis Composite.

Characterization of Collagen (Bovine Collagen Peptide) by Electron Microscopy (SEM)

Collagen *(Bovine Collagen Peptide*) samples are also characterized using Electron Microscopy (SEM) Spectroscopy to see the particle surface morphology or the 3-dimensional shape of the particle and the size of the particle. Scanning Electron Microscopy (SEM) has a magnification of 10-3,000,000x so that it can produce detailed surface images. SEM analysis of Collagen Samples (*Bovine Collagen Peptide*) that has been performed at a magnification of 20,000x and 40,000x can be seen in Figure 10.

Based on the results of SEM with magnifications of 20,000x and 40,000x in Figure 10, it can be seen that the particle morphology of pure collagen samples is spherical in shape with pores that appear small and the surface is flat and smooth and the particle distribution is uniform. Uniformity and pore size are some of the main factors to determine collagen quality. Thus, it can be concluded that bovine collagen peptide is successfully synthesized and has the potential to be used as a biomaterial in its composite with hydroxyapatite compounds such as bone grafts or scaffolds for bone tissue engineering and other medical applications.

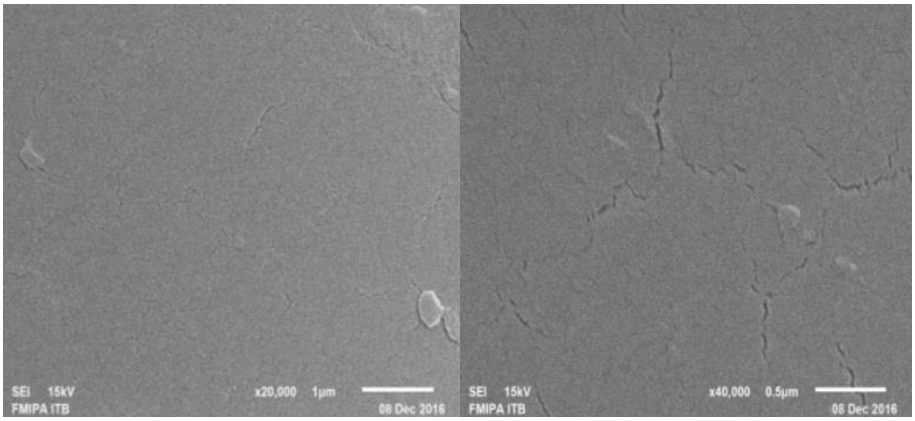

(a) (b)

FIGURE 10 Morphology of Collagen (*Bovine Collagen Peptide*) SEM test results (a) magnification 20,000x and (b) magnification 40,000x

Hydroxyapatite and collagen nano composites

Making collagen-hydroxyapatite composites was done using chemical methods in accordance with the method of [13] with several modifications. The collagen and hydroxyapatite to be made composite are first dissolved in a solvent. When two materials are combined in the form of a solution, a chemical bond will occur.

Bone consists of intracellular components in the form of cells including osteoprogenitors, osteoblasts, osteocytes, osteoclasts and extracellular matrix components, namely, the organic matrix of bone by 33% consists of Type I collagen, and the inorganic matrix of bone by 67% which is composed of hydroxyapatite ($Ca_{10}(PO_4)_6(OH)_2$) [27]. In this study, the mass ratio of HAp: Collagen composition was 67: 33.

Collagen is mixed with acetic acid and Na_2HPO_4. H_2O with a ratio of b/v/b is 1/1/1. All ingredients are stirred perfectly. The addition of acetic acid is intended to dissolve collagen. Collagen dissolves well in acetic acid, but collagen can actually dissolve in water with a low solubility level. While the addition of Na_2HPO_4. H_2O aims to condition the sample to a state of equilibrium of body fluids. Na_2HPO_4. H_2O is a PBS (Phosphate Buffer Saline) fluid whose composition is similar to body fluids. After the sample is thoroughly mixed, 1 M NaOH is added to neutral pH to precipitate liquid collagen.

Powdered hydroxyapatite is mixed with phosphoric acid (H_3PO_4) with a w/v ratio of 1/4. This comparison aims so that hydroxyapatite can dissolve perfectly in phosphoric acid. Then NH_4OH is added until the pH is neutral. Phosphoric acid is commonly used in the manufacture of synthetic hydroxyapatite. The solution of Collagen and Hydroxyapatite is mixed and stirred, and then incubated for ± 6 hours.

The sample is then freeze-dried (Figure 11). Hydroxyapatite-Collagen composite has very hygroscopic properties, so it must be stored in a cool and dry place. If left in open air conditions then the composite will be wet, sticky, and turn yellowish.

FIGURE 11 Precipitation of Collagen-Hydroxyapatite composite solution

Characterization of Hydroxyapatite-Collagen Nanocomposites with X-Ray Diffraction (XRD)

Analysis of XRD characterization results was carried out with intensity from peaks on diffractograms measured by databases. The synthesized $Ca_{10}(PO_4)_6(OH)_2$ compound matched with JCPDS 09-0432 data can be seen in Figure 12.

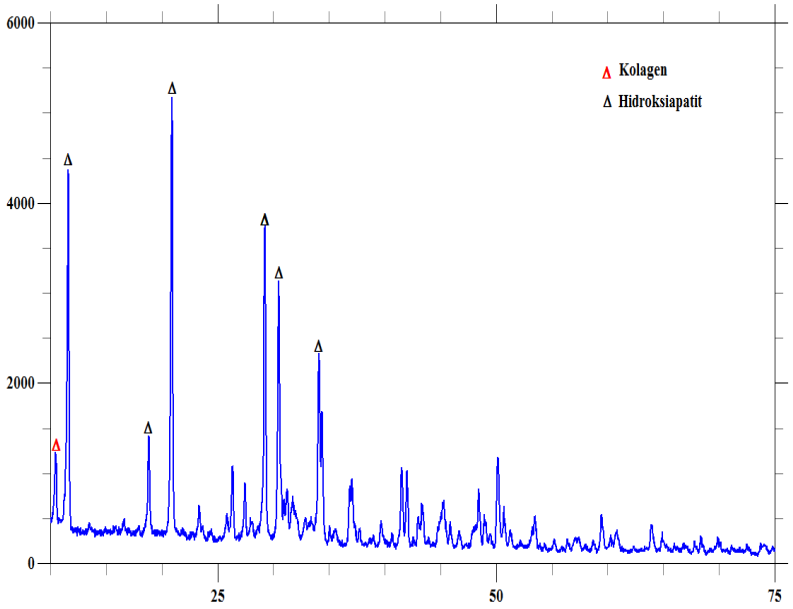

FIGURE 12 HAp-Collagen composite XRD pattern

Based on the XRD pattern for HAp-Collagen composite samples, the phase formed is Hap, and the joint peak of collagen and HAp appears at an angle of 2θ 10.45°. The appearance of collagen-owned peaks in the HAp-Collagen composite signifies that HAp has filled the collagen matrix. There is a low intensity of collagen because collagen has spread in the HAp sample indicating that collagen has bound to hydroxyapatite.

Characterization of Hydroxyapatite-Collagen Nanocomposites with Fourier Transform Infra-Red (FTIR)

The FTIR spectra of the HAp-Collagen composite show all the characteristic peaks of collagen with additional HAp peaks given in Figure 13. The graph of FTIR test results is analyzed by comparing the absorption bands formed in the infrared spectrum using a correlation table. The results of the comparison of absorbs bands are presented in Table 5.

TABLE 5 Absorption characteristics of collagen-hydroxyapatite composites [28]

No.	Wavenumber Range (cm^{-1})	Peak (cm^{-1})	Bond
1.	3640-3160	3232	O-H
2.	3000-2500	3081	O-H
3.	2960-2850	2873	C-H
4.	2260-2100	2202	C-=C
5.	1760-1670	1716	C=O
6.	1700-1600	1672	N-H
7.	1600-1500	1519	N-H
8.	1470-1350	1460	C-H
9.	1470-1350	1405	C-H
10.	1340-1020	1200	C-N
11.	1340-1020	1074	C-N
12.	1200-900	1018	PO_4^{3-}
13.	1200-900	966	PO_4^{3-}
14.	600-500	553	C-X

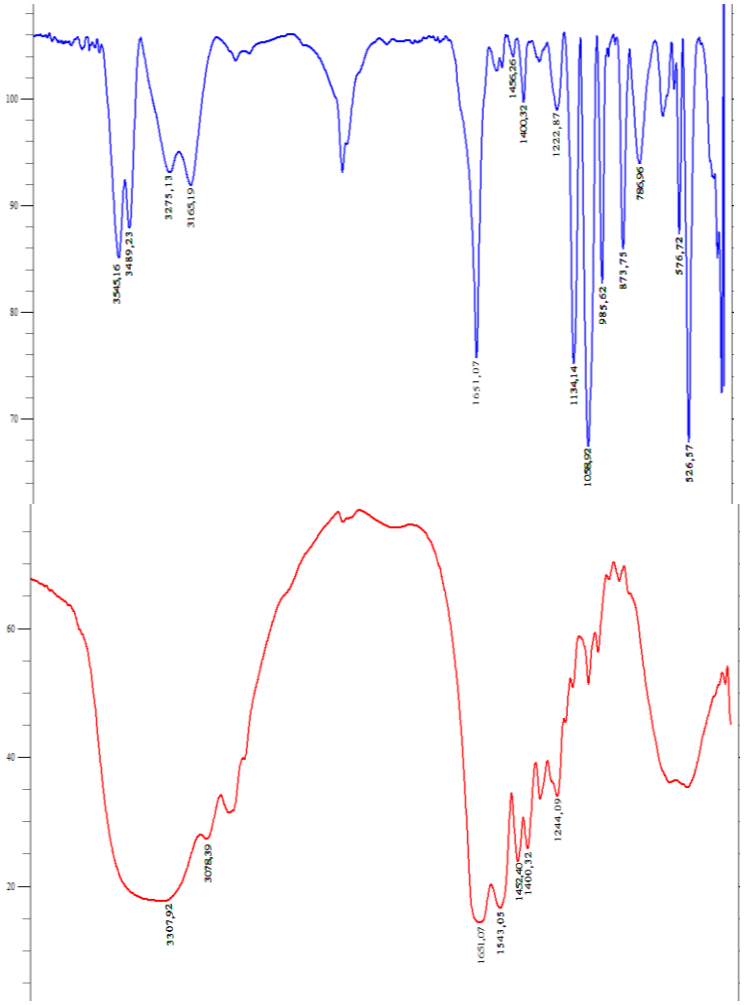

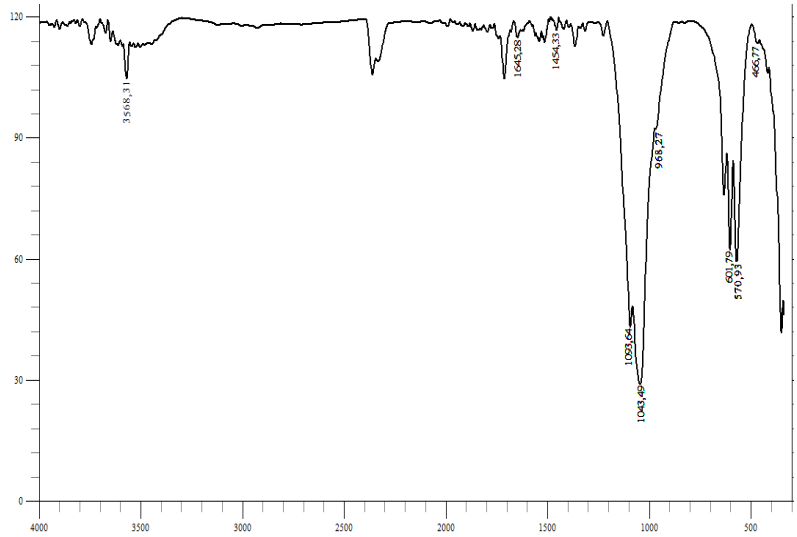

FIGURE 13 FTIR spectroscopic spectroscopy of HAp-Collagen (*Bovine Collagen Peptide*) nanocomposites

Figure 13 demonstrates the FTIR absorption band of the entire sample. The IR spectrum from the sample showed the presence of phosphate absorption bands for symmetrical vibrational stretching (υ_1), *asymmetric vibration stretching* (υ_3), bending asymmetry vibration (υ_4), and symmetrical vibrational carbonate absorption band *bending* (υ_2), as well as hydroxyl absorption, bands the appearance of the three groups, indicates the formation of HAp. The phosphate absorption band$_{\upsilon 1}$ appears at wavenumbers 985.62 cm^{-1}, υ_3 appears at wavenumbers 1058.92 cm^{-1} and 1134.14 cm^{-1}. While the phosphate group$_{\upsilon 4}$ appears at wavenumbers 526.57 cm^{-1}, 576.72 cm^{-1}, and 786.96 cm^{-1}. The hydroxyl group in the HAp sample appears at wavenumbers 3489.23 cm^{-1} and 3545.16 cm^{-1}. The carbonate absorption band υ_2 is present at wavenumber 873.75 cm^{-1}.

The picture also shows the FTIR absorption band in HAp + Collagen composite samples has formed C-H, C-N, N-H, and C=O groups which are characteristic of collagen. In HAp + Collagen composite samples, the N-H Groups are stacked with OH^- Groups so that the absorption band of FTIR spectra looks wider in the wavenumber regions of 3545.16 cm^{-1} and 3489.23 cm^{-1}. C-H groups also appear in HAp+K composite samples. C-H groups appear at wavenumbers 1400.32 cm-1, 1456.26 cm^{-1}, 3275.13 cm^{-1}, and 3165.19 cm^{-1}. The C=O group in the composite sample appears in the 1651.07 cm^{-1} waybill. The C-N group appears at wavenumber 1222.87 cm^{-1}. The presence of HAp functional groups and N-H, C-H, C-N, and C=O groups in HAp + Collagen composite samples which are characteristic of collagen indicates that collagen has bound to apatite and HAp + Collagen composites have been successfully formed. This can be seen from the spectral form in Table 5.

Hydroxyapatite-Collagenc omposite synthesized using *the freeze-drying* method by freezing at -40 ^{o}C for 24 hours is seen in Figure 14.

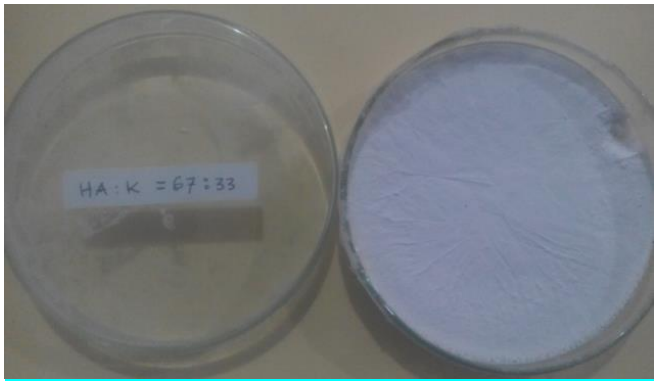

FIGURE 14 Hydroxyapatite-Collagen composite

The bond that allows Hydroxyapatite to occur between hydroxyapatite and collagen is a hydrogen bond because collagen includes proteins and hydroxyapatite is ceramic. Hydrogen bonding is a molecular bonding mechanism. Hydrogen bonding indicates that the crosslinking that occurs is a bond between hydrogen atoms with one electronegative atom and is attracted toward another electronegative atom. The molecular bonding mechanism that is possible in this study is that hydrogen bonding occurs between the H atom owned by collagen and the O atom in hydroxyapatite.

Functional group absorption data in the FTIR spectrum is also used to determine the type of reaction that occurs. If the data coincides with the FTIR spectral data of the material used, then the process that occurs is a physical process. Meanwhile, if the data does not converge, the process that occurs is a chemical reaction. Based on the comparison of the results of FTIR hydroxyapatite, collagen, and hydroxyapatite-collagen composites, the reaction that occurs in the synthesis process of hydroxyapatite-collagen composites is a chemical reaction [27].

Mixing hydroxyapatite with collagen results in collagen being mineralized by hydroxyapatite. Mineralized collagen occurs due to the interaction that arises between the structure of collagen and hydroxyapatite crystals. In fact, such interactions occur between carboxylate groups and $Ca2^{+}$ cations, which can be illustrated in Figure 15. This hypothesis is supported by FTIR data which is explained based on the C-O spectrum and C=O band in pure collagen and collagen-hydroxyapatite composites as well as mesomeric carboxylate anions forming stabiL carboxylate ions.

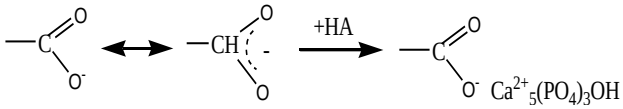

FIGURE 15 The mesomeric form of the carboxylate group is stable during mineralization

The result of such interaction is that hydroxyapatite particles are perfectly deposited on collagen fibers. This supports the nucleation between collagen and hydroxyapatite. This nucleation center can be clearly seen in the SEM result image.

Characteristics of Hydroxyapatite-Collagen Nanocomposites by Electron Microscopy (SEM)

The results of the *Electron Microscopy (SEM) Spectroscopy* (SEM) image in Figure 16 with magnifications of 20,000x and 40,000x show macroporous morphological shape, pore size, surface roughness, and pattern of combining hydroxyapatite with collagen in the synthesized composite.

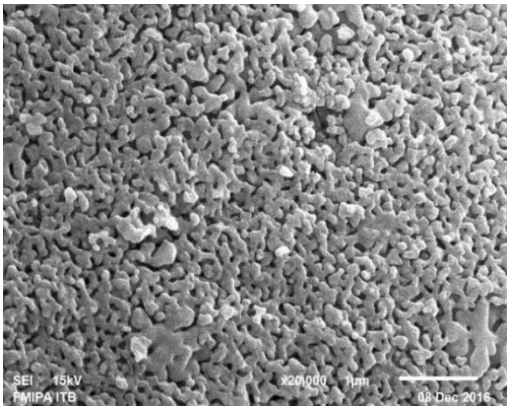

(a)

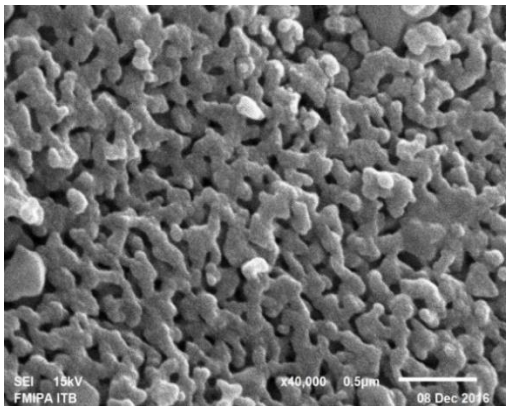

(b)

FIGURE 16 Morphology of Hydroxyapatite-Collagen nanocomposites SEM test results (a) magnification 20,000x and (b) magnification 40,000x

The results of the SEM test show hydroxyapatite attached to collagen fibers which shows that a hydroxyapatite-collagen composite has been formed, where collagen acts as a matrix where apatite grows. The hydroxyapatite particles in the composite spread uniformly, visible through the collagen matrix that has been interconnected between cells. The shape of the pores noticeably changed compared to the HAp sample itself, in the pure collagen sample the pores were flatter, and when HAp merged with collagen the pores looked more rounded. In Figure 16, collagen fibers act as composite fibers, and hydroxyapatite act as a composite matrix. The nucleation centers of collagen with hydroxyapatite can be seen, but are not evenly distributed on all surfaces. Uneven nucleation of collagen with hydroxyapatite is caused by hydroxyapatite not being evenly deposited on collagen fibers. Macro-wise, the composite surface looks smooth.

Conclusion

Based on the results of the research that has been done, the following conclusions can be drawn:

1. Hydroxyapatite-collagen composites have been successfully synthesized by ***freeze-drying*** method. Control of freezing time with a temperature of 40 ^{o}C for 24 hours resulted in a combination of collagen and HAp in the composite blended well.
2. Based on the composite XRD pattern, HAp-Collagen joint peaks belong to collagen and HAp appear at an angle of 2θ 10.45°, indicating HAp fills the collagen matrix. FTIR characterization shows the presence of PO_4^{3-} and OH^- absorption bands of HAp, as well as wavenumber shifts in C-H, C-N, N-H, and C=O groups that are characteristic of collagen. SEM characterization shows HAp is perfectly deposited into collagen molecules.

Acknowledgments

We thank the Central Laboratory of Padjadjaran University and the Inorganic Laboratory of Hasanuddin University for their support of this research.

Funding

Grant funding for this research was provided by the Hasanuddin University Research and Community Service Institute through the Collaborative Fundamental Research plan for the Fiscal Year 2023 by contract number 00323/UN4.22/PT.01.03/2023.

Authors' Contributions

Maming Maming, Fadliah Mubakira, and Indah Raya Idea generation, Research, Technique, and Original Draft Writing. Bulkis Musa, Andi Muhammad Anshar, and Erna Mayasari Writing, editing, review, and Validation. Yusafir Hala, Syaharuddin Kasim, Andi Ilham L., and Gemini Alam Writing, editing, and review. Andi Nilawati Usman, Hasmawati, Hasri, Andriani Usman, and Rizal Irfandi Created the Figures and Tables.

Conflict of Interest

The authors declare that they have no conflicts of interest.

Orcid:

Indah Raya:
https://orcid.org/0000-0001-8575-1994
Bulkis Musa:
https://orcid.org/0009-0004-6132-310X
Andi Muhammad Anshar:
https://orcid.org/0000-0003-1055-240X
Erna Mayasari:
https://orcid.org/0000-0002-8021-1478
Andi Nilawati Usman:
https://orcid.org/0000-0002-1136-1704
Hasri Hasri:
https://orcid.org/0000-0003-3353-3789
Rizal Irfandi:
https:www.orcid.org/0000-0002-4845-3397

References

[1] M. Chandran, K. Brind'Amour, S. Fujiwara, Y-C. Ha, H. Tang, J-S. Hwang, J. Tinker, J.A. Eisman , Prevalence of osteoporosis and incidence of related fractures in developed economies in the Asia Pacific Region: a systematic review, *Osteoporos Int.,* **2023**, *34*, 1037–1053. [Crossref], [Google Scholar], [Publisher]

[2] M. Sivakumar, T.S. Sampath Kumar, K.L. Shanta, R.K. Panduranga. Development of hydroxyapatite derived from Indian coral, *J. Biomater.*, **1996**, *17*, 1709-1714. [Crossref], [Google Scholar], [Publisher]

[3] A). E. Garetta, T. Fernandez, S. Borros, J. Esteve, C. Colominas, L. Kempf, Synthesis of biocompatible surfaces by different techniques, *J. Mat. Res. Soc. Symp. Proc,* **2002**, *724*, N8.11.1-N8.11.6. [Crossref], [Google Scholar], [Publisher] b). R. Kareem, N. Bulut, O. Kaygili, Hydroxyapatite biomaterials: a comprehensive review of their properties, structures, medical applications, and fabrication methods, *J. Chem. Rev.*, **2024**, *6*, 1-26. [Crossref], [Pdf], [Publisher]

[4] a). C.D. Nascimento, Biomaterials applied to the bone healing process, *Int. J. Morphology*, **2007**, *25*, 839-846. [Google Scholar], [PDF] b). B. Khatri, A. Rajbhandari (Nyachhyon), Preparation, characterization and photocatalytic application of novel bismuth vanadate/hydroxyapatite composite, *Adv. J. Chem. A.*, **2020**, 789-799. [Crossref], [Google Scholar], [Publisher] c). A.A. Radhi, H. Aljudy, The impact of mixed NaOH and KOH mole fraction on mechanical performance of metakaolin based geopolymer material, *J. Med. Chem. Sci.*, **2023**, *6*, 1120-1128. [Crossref], [Pdf], [Publisher] d) H.A. Ameer Radhi, M. Abdulaziz Ahmad, Biological test of porous geopolymer as a bone substitute, *J. Med. Chem. Sci.*, **2023**, *6*, 710-719. [Crossref], [Google Scholar], [Publisher]

[5] S. Ahmed, M. Ahsan, Synthesis of Ca-hydroxyapatite bioceramic from egg shell and its characterization, *Bangladesh J. Sci. Ind. Res.*,

2008, *43*, 501-512. [Google Scholar], [Publisher]
[6] T.Q. Abd Alkareem, E.J. Waheed. Formation, characterization and antioxidant study of mixed ligand complexes derived from succinyl chloride, *Chem. Methodol.*, **2022**, *6*, 914-928. [Crossref], [Pdf], [Publisher]
[7] A.E. Ahmed Tamer, W. Ling, Y. Manar, H. Maxwell, Biotechnological applications of eggshell: recent advances, *J. Front. Bioeng. Biotechnol.*, **2021**, *9*. [Crossref], [Google Scholar], [Publisher]
[8] G. Ahlborn, B. W. Sheldon, Identifying the components in eggshell membrane responsible for reducing the heat resistance of bacterial pathogens, *J. Food Prot.*, **2006**, *69,* 729-38. [Crossref], [Google Scholar], [Publisher]
[9] S.F. Bao, W. Windisch, M. Kirchgessner, Calcium bioavailability of different organic dietary source (citrate lactate, acetate, oyster-shell, eggshell, calcium phosphate), *In J. Anim. Physiol. Anim. Nutr.*, **1997**, *78*, 154-160. [Crossref], [Google Scholar], [Publisher]
[10] H.C. Elliott, P.E. Mackie, R.A. Young, Monoclinic hydroxyapatite, *Science*, **1973**, *180*, 1055-1057. [Crossref], [Google Scholar], [Publisher]
[11] T.S.B. Nasaraju, D.E. Phebe, Some physico-chemical aspects of hydroxylapatite, *J. Mat. Sci.*, **1966**, *31*, 1-21. [Crossref], [Google Scholar], [Publisher]
[12] W. Wang, K.W.K. Yeung, Bone grafts and Biomaterials Substitutes for Bone Defect Repair: a review, *Bioact. Mater.*, **2017**, *2*, 224-247. [Crossref], [Google Scholar], [Publisher]
[13] T.T. Roberts, A.J. Rosenbaum, Bone grafts, bone substitutes and orthobiologics: the bridge between basic science and clinical advancements in fracture healing, *Organogenesis*, Oct-Dec., **2012**, *8*, 114-124. [Crossref], [Google Scholar], [Publisher]
[14] N.A.S. Mohd Pu'ad, J. Alipal, H.Z. Abdullah, M.I. Idris, T.C. Lee. Synthesis of Eggshell Derived hydroxyapatite via chemical precipitation and calcination method, *Materials Today: Proceedings*, **2021**, *42*, 172-177. [Crossref], [Google Scholar], [Publisher]
[15] N.D Malau, F. Adinugraha. Synthesis of hydrokxyapatite based duck egg shells using precipitation method, *J. Phys.: Conf. Ser.,* **2020**, *1563*, 012020. [Crossref], [Google Scholar], [Publisher]
[16] Albuquerque, C.G. Monica, I. Jimenez-Urbistondo, J. Santamaria-Gonzalez, CaO supported on mesoporous silicas as basic catalysts for transesterification reactions, *Appl Catal A: Gen*, **2008**, *334*, 35-43. [Crossref], [Google Scholar], [Publisher]
[17] M.C. Reis, M.F.B. Sousa, F. Alobaid, C.A. Bertran, Y. Wang, A two-fluid model for calcium carbonate precipitation in highly supersaturated solutions, *Adv. Powder Technol.*, **2018**, *29*, 1571-1581. [Crossref], [Google Scholar], [Publisher]
[18] P. Agrinier, A. Deutsch, U. Scharer, I. Martinez, Fast back-reactions of shock-released CO_2 from carbonates: an experimental approach, *Geochim. Cosmochim. Acta.*, **2001**, *65*, 2615-2632. [Crossref], [Google Scholar], [Publisher]
[19] M.L. Granados, M.D. Poves, D.M. Alonso, R. Mariscal, F.C. Galisteo, T.R. Moreno, J. Santamaría, L.G. Fierro, Biodiesel from sunflower oil by using activated calcium oxide, *Appl. Catal. B: Environ.*, **2007**, *73*, 317-326. [Crossref], [Google Scholar], [Publisher]
[20] R. Han, Y. Wang, S. Xing, C. Pang, Y. Hao, C. Song, Q. Liu, Progress in reducing calcination reaction temperature of calcium-looping CO_2 capture technology: a critical review, *J. Chem. Eng.*, **2022**, *450*, 137952. [Crossref], [Google Scholar], [Publisher]
[21] K. Dahlan, F. Prasetyanti, Y.W. Sari, Synthesis of hydroxyapatite from eggshells using dry method, *J. Biophysics*, **2009**, *5*, 71-78. [Google Scholar]
[22] H. Pan, B.W. Darvell, Effect of carbonate on hydroxyapatite solubility, Crystal Growth & Amp; *Design*, **2010**, *10*, 845-850. [Crossref], [Google Scholar], [Publisher]
[23] N.A. Luchman, A.W.R. Megat, S.H.Z. Ariffin, N.S. Nasruddin, S.F. Lau, F.Yazid, Comparison

between hydroxyapatite and polycaprolactone in inducing osteogenic differentiation and augmenting maxillary bone regeneration in rats, *PeerJ*., **2022**, *10*, e13356. [Crossref], [Google Scholar], [Publisher]

[24] M. Ozawa, S. Suzuki, Microstructural development of natural hydroxyapatite originated from fi sh-bone waste through heat treatment, *J. Am. Ceram. Soc.,* **2002**, *85*, 1315-1317. [Crossref], [Google Scholar], [Publisher]

[25] R. Pallela, J. Venkatesan, S.K. Kim, Polymer assisted isolation of hydroxyapatite from *Th unnus obesus* bone, *J. Ceram. Int.,* **2011**, *37*, 3489-3497. [Crossref], [Google Scholar], [Publisher]

[26] S. Kirubanandan, P.K. Sehgal, Regeneration of soft tissue using porous bovine collagen scaffold, *J. Optoelectron. Biomed. Mate.*, **2010**, *2*. [Google Scholar], [PDF]

[27] X. Feng, Chemical and biochemical basis of cell-bone matrix interaction in health and disease, *Curr Chem Biol*., **2009**, *3,* 189-196. [Crossref], [Google Scholar], [Publisher]

[28] M.Z. Ichsan, Synthesis of collagen-hydroxyapatite composite macroporus as a bone graft candidate, *Thesis*, Department of Physics, Faculty of Science and Technology, Airlangga University: Surabaya., **2012** [Crossref]

How to cite this article: Maming Maming, Fadliah Mubakira, Indah Raya, Bulkis Musa, Andi Muhammad Anshar, Erna Mayasari, Yusafir Hala, Syaharuddin Kasim, Andi Ilham L., Gemini Alam, Andi Nilawati Usman, Hasmawati Hasmawati, Hasri Hasri, Andriani Usman, Rizal Irfandi, Fabrication and analysis of nano-hydroxyapatite [$Ca_{10}(PO_4)_6(OH)_2$] composites with collagen derived from eggshells through freeze-drying. *Journal of Medicinal and Pharmaceutical Chemistry Research*, 2023, 5(12), 1173-1193. **Link:** http://jmpcr.samipubco.com/article_182241.html